Control of plasmonic wave propagating in nanocavity with tooth-shaped configuration*

Li Xu-Feng(李旭峰), Pan Shi(潘 石)†, Guo Ying-Nan (郭英楠), and Wang Qiao(王 乔)

School of Physics and Optoelectronic Technology, Dalian University of Technology, Dalian 116024, *China*

(Received 24 April 2010; revised manuscript received 6 July 2010)

Characteristics of plasmonic wave propagating in nanocavity formed by two silver films are studied numerically. The groove etched inside wall of the top film makes it possible to control the propagation when light goes through the top film along a nanoslit into the cavity. It is found that the transmission wave through the channel of groove etched side can be filtered linearly with the groove of a certain depth; while the other side is still open for this wave and its intensity can be enhanced periodically with the variable groove position in both films, which are explained well based on the interference of plasmonic waves in the system.

Keywords: plasmonic wave, optical devices, FDTD

PACS: 52.35.–g, 42.79.–e, 02.60.–x **DOI:** 10.1088/1674-1056/20/1/015204

1. Introduction

Surface plasmon polaritons (SPPs) are light waves coupled to free electron oscillations in metal/dielectric interface. Both theoretical and experimental studies have proved that the dispersion of SPPs can be improved for special demands[1,2] by modifying the interface. With the merits of such an improvement, one can concentrate the light beams beyond the diffraction limit or guide the light through a subwavelength aperture efficiently. Since the first observation of extraordinary optical transmission through a metallic film with nanohole arrays,[3] light propagating on the tiny scale has greatly aroused people's interest[4] and developed in many branches, such as miniaturized devices of waveguides,[5] filters,[6,7] combiners,[8] couplers[9] and splitters,[10] all of which are based on the control of SPP propagation and intensity.

With regard to the control of SPPs, several groups have proposed many constructive methods. By adding different nano-structures to both sides of the nanoslit, a device capable of controlling SPPs propagation in opposite directions has been proposed by Gan *et al.*[11] and they have also investigated the bidirectional subwavelength splitters for SPPs in THz and near infrared domain with the similar structures.[12,13] Metal grating with a subwavelength aperture used for handle SPP direction and splitting are mentioned in Refs. [14] and [15]. In addition to the researches of SPP transmission in single nanoslit, the cases in slit array are also concerned. Verslegers *et al.*[16] have confirmed that the direction control of SPPs is feasible by changing metallic nanoslit array width and period. In general, such a control can be classified into two factors: one is the phase control based on the modified structure and the other is the intensity. Controlling SPP phase and amplitude has been studied by subwavelength dielectric slits or the cavities embedded in a metal slab,[17,18] and the authors have also demonstrated that the Fabry–Perot (F–P) resonance plays an important role in the process. In accordance with the same resonance, a device for the controlling and splitting of SPPs is reported by Wang *et al.*[19] In addition, the SPPs can also be modulated by the incident wave intensity.[20] All these studies have greatly promoted the applications of SPPs in practice and attracted the researchers for further study in such fields.

In this paper, a special device capable of controlling SPP propagation and intensity in nanocavity is proposed by etching a groove in the top film (film 1). Numerical simulations show that such a manipulation is possible when the groove shape and position are changed. The control by etching the groove in film below (film 2) is also considered and its function is found to be similar to that in film 1, in a sense, which makes the design to be more practical as film 2 is moved together with the groove. In this way, the SPP sources and intensity can be tuned efficiently.

*Project supported by the National Natural Science Foundation of China (Grant No. 10974025).

†Corresponding author. E-mail: span@dlut.edu.cn

© 2011 Chinese Physical Society and IOP Publishing Ltd

2. Model and method

Structure of the system is depicted in Fig. 1, which consists of two metallic films with different values of thickness t_t for film 1 and t_b for film 2. The tooth-like groove with depth h, width W is etched only on one side of film 1. Parameters of $t_t = 390$ nm, $t_b = 300$ nm, $W_p = 1750$ nm and $W_s = 25$ nm are similar to those in Ref. [19]. For exciting SPPs at the metal/air interface efficiently, a p-polarized plane wave impinges normally onto the structure. The SPPs confined in the interface propagate along it, go through film 1 along the nanoslit into a horizontal channel splitting into two parts.

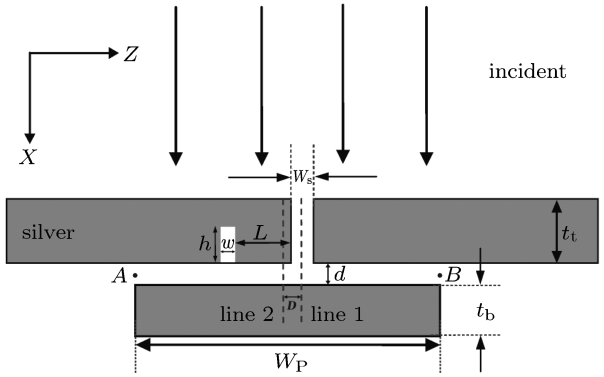


Fig. 1. Schematic diagram of control system.

In channel exits, the SPP intensity is related to groove position L and shape. Lines 1 and 2 denote the central axes of films 1 and 2 respectively. Position of film 2 is kept right beneath film 1 with a distance d for $D = 0$ nm, thus the channel can be regarded as two metal–insulator–metal (MIM) waveguides. Points A and B are set in the centre of exits to monitor the variation of z-component magnetic field H_z. Both films 1 and 2 are of sliver with a permittivity of $\varepsilon_m = -48.8 + \mathrm{i}\,3.16$ at $\lambda_0 = 1000$ nm. The frequency-dependent permittivity of sliver is characterized by the Drude model and the parameters are given in Ref. [19].

We consider that the structure is infinite in the y-axis, so the system can be simplified into a two-dimensional system. The complex propagation constant β in the MIM waveguide is given by

$$\begin{aligned} &\varepsilon_d\sqrt{\varepsilon_m k_0^2 - \beta^2} + \varepsilon_m\sqrt{\varepsilon_d k_0^2 - \beta^2} \\ &\times \coth(-\mathrm{i}\sqrt{\varepsilon_d k_0^2 - \beta^2} w_{slit}/2) = 0, \\ &\beta = \mathrm{Re}(n_{eff})k_0. \end{aligned} \tag{1}$$

Herein, symbols k_0, ε_m, ε_d, w_{slit}, and n_{eff} are defined respectively as the wave vector of incident light in vacuum, the metal permittivity, the permittivity of medium filled in the waveguide, the width of waveguide, and the refractive index of SPP. A finite-difference time-domain (FDTD) method[21] is adopted to calculate the field distribution of H_z. The mesh size is 2.5 nm×2.5 nm, which is smaller than the fine feature of the model to ensure the accuracy of results. A perfectly matched layer (PML) at the computational boundaries is used to absorb the outgoing electromagnetic waves.

3. Results and discussion

A vertical MIM waveguide of finite length is formed by a nanoslit milling in film 1, and the F–P resonance occurs in the narrow region according to the effective wavelength in such a waveguide.[22] The light transmission through the slit is maximal due to constructive interference for a length phase of even integral multiple of $\pi/2$ and minimal for a length phase of odd integral multiple of $\pi/2$. Therefore the thickness of film 1 should be selected carefully for concentrating more energy into the horizontal channel. Parameters, not mentioned previously, are $w = 25$ nm, $h = 130$ nm and $d = 45$ nm.

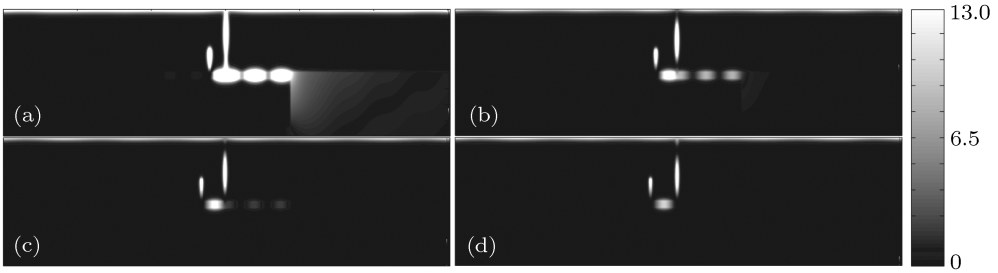


Fig. 2. $|H_z|^2$for different L : (a) 195 nm, (b) 260 nm, (c) 295 nm and (d) 335 nm.

Figures 2(a)–2(d) show the time-averaged field intensity distributions of $|H_z|^2$ for different values of L. There are two cases that should be noticed from the results. (i) The groove in channel A can work as a lock to block the SPP transmission through it, while channel B is still open; (ii) the SPP intensity in port B can be changed with L. A maximal value is obtained for $L = 195$ nm in Fig. 2(a) and a minimal value for $L = 335$ nm in Fig. 2(d).

Figures 3(a) and 3(b) represent $|H_z|^2$ at points A and B, each as a function of the groove depth for L ranging from 25 nm to 335 nm. It can be seen from Fig. 3(a), the depth for the minimal $|H_z|^2$ is invariable, irrespective of L, which becomes active only if the L is too small to enable SPP to penetrate through the slit wall into the groove, then the SPPs interaction between them occurs, resulting in the depth less than 130 nm. Comparing Fig. 3(a) with Fig. 3(b), one can find that the SPP intensity in port A is suppressed, while that in port B can be enhanced by changing L. For $L = 195$ nm, the intensity in port B is 80 times larger than that in port A and 2.53 times larger than that in the case of no groove. For $L = 335$ nm, the ports are both locked. Based on the interference of plasmonic waves in such waveguides, such phenomena are explained as follows.

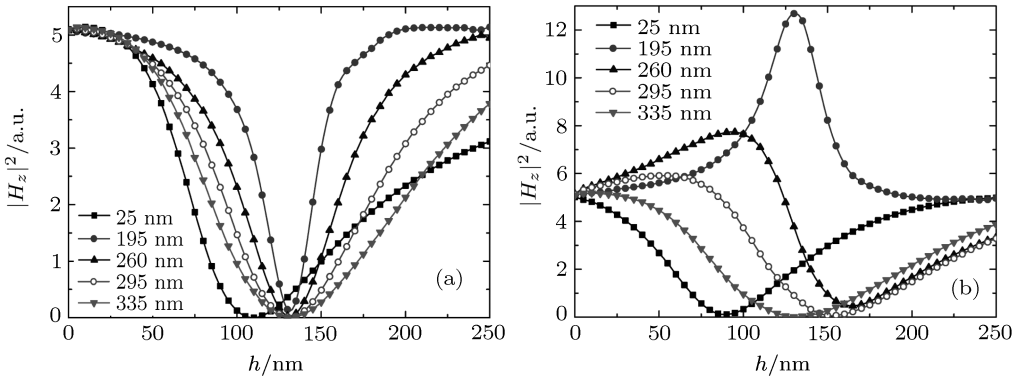


Fig. 3. $|H_z|^2$ at points A (a) and B (b) with the variation of groove depth for different values of L.

SPPs transmit in the horizontal channel, split two branches propagating along the opposite directions. When the left branch is blocked by the groove, it reflects to couple with the right one flowing into channel B. The phase difference between them can be written as

$$\varphi = 2\pi n_{\rm eff}^{\rm c} \cdot 2L/\lambda_0 + \Delta\varphi, \tag{2}$$

where $n_{\rm eff}^{\rm c}$ is the refractive index of SPP in the horizontal channel, which is determined by Eq. (1), and $\Delta\varphi$ represents the phase shift aroused by the reflected SPP at the metal/air segments of groove and slit in film 1. By taking channel B as an F–P cavity, the intensity in port B can be calculated from the following formula:

$$S = \left| \frac{A_0 T_{\rm r}^1 T_{\rm r}^2}{1 - R_{\rm r}^1 R_{\rm r}^2 + 4\sqrt{R_{\rm r}^1 R_{\rm r}^2}\sin^2(\phi/2)} \right|, \tag{3}$$

where parameters $T_{\rm r}^1$, $T_{\rm r}^2$, $R_{\rm r}^1$, and $R_{\rm r}^2$ are respectively the transmittances and reflectances at both ends of channel B whose length is $W_{\rm pr}$ ($\phi = 4\pi n_{\rm eff}^{\rm c} W_{\rm pr}/\lambda_0$); A_0 denotes the coupled intensity of the two branches mentioned above in threshold of channel B, which is related to, owing to the interference of them. Changing L or h, A_0 is affected, thereby S varies. The period of S in Fig. 4(a) for changing L is found to be similar to that for moving film 2 in Fig. 4(b). The period calculated by FDTD accords well with the theoretical predication of 344.8 nm for $n_{\rm eff}^{\rm c} = 1.42$ from the item $\sin^2(\phi/2)$, then Eq. (3) can be rewritten in the following form:

$$S = \left| (I_{\rm l} + I_{\rm r} + 2\sqrt{I_{\rm l} I_{\rm r}}\cos(\varphi)) \times \frac{T_{\rm r}^1 T_{\rm r}^2}{1 - R_{\rm r}^1 R_{\rm r}^2 + 4\sqrt{R_{\rm r}^1 R_{\rm r}^2}\sin^2(\phi/2)} \right|. \tag{4}$$

Parameters $I_{\rm l}$ and $I_{\rm r}$ are the SPP intensities reflected by groove and transmitted directly into channel B respectively. Supposing that $I_{\rm l}$, $I_{\rm r}$,$T_{\rm r}^1$, $T_{\rm r}^2$, $R_{\rm r}^1$, and $R_{\rm r}^2$ are constants, the same periods of S for varying L and $W_{\rm pr}$ can be proved by Eq. (4). In contract to the case in Fig. 4(a), moving film 2 in Fig. 4(b)

has no contribution to the enhancement of SPPs and also does not filter the transmission wave completely in both channels A and B. For the minimal intensity, its value is still larger than 0.5. However, taking the groove into consideration, it is another story. When L meets the condition of $\varphi = (2m+1)\pi$, $m = 0, 1, 2\ldots$, the minimal S is obtained and becomes zero given $|I_{\rm l} - I_{\rm r}| \to 0$ in Fig. 4(a); for $\varphi = 2m\pi$, S is enhanced maximally. In addition, it can be found from the figure that the difference between the two curves of groove in films 1 and 2 is too faint to be distinguishable for $L > 60$ nm, thus, the device of groove in film 2 becomes more practical as it is moved. In the way, given the groove etched right beneath the slit exit of film 1, tunable SPP sources in ports A and B can be realized by moving film 2. Moreover, the intensity can be further enhanced by optimizing the length of film 2 for the F–P resonance produced in both channels A and B.

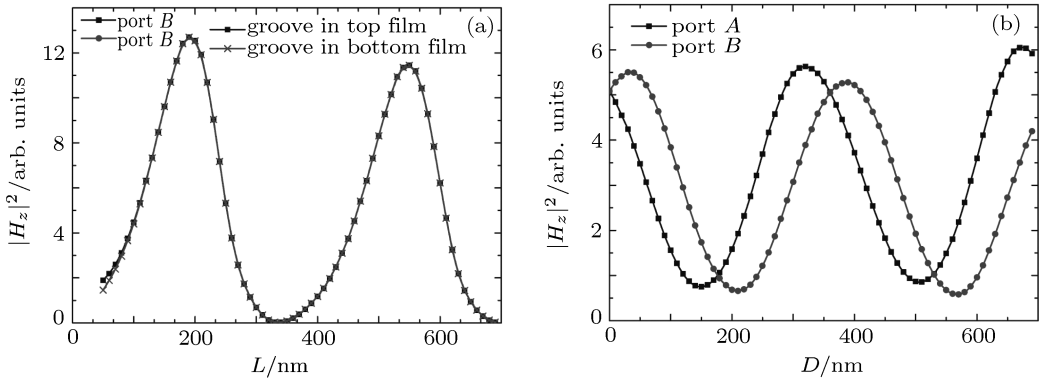


Fig. 4. (a) $|H_z|^2$ versus L in port B, (b) $|H_z|^2$ in ports A and B versus D, where D is the relative position between the top and bottom films.

Controlling SPP propagation and intensity by changing groove position and depth has been studied, from which we know that the transmission wave in channel A can be filtered with the groove of certain depth. Furthermore, the depth-dependent filtered wavelength with the variable groove width and the distance between films 1 and 2 is also concerned. The discrete points in Fig. 5 represent the calculated results by FDTD, and the straight lines refer to the fitting curves.

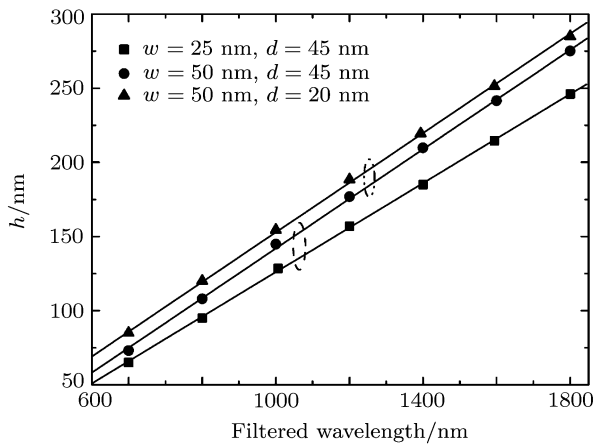


Fig. 5. Filtered wavelengths versus groove depth in port A.

Curves encircled by the dash dot–dot line represent the groove with the same width of $w = 50$ nm and different distances: $d = 20$ nm and 45 nm; while the opposite cases of $w = 25$ nm, 50 nm and $d = 45$ nm are encircled by the dash lines. Each of them shows a linear response. The deeper the groove is, the longer can the filtered wavelength be. The filtered wavelength is a function of the groove depth, width and the distance between the films, which can be interpreted well by Eq. (6).

Some parts of the transmission SPP in channel A which reaches the position of groove etched, go around the groove, while the others propagate directly. When they meet again, the phase shift is described as

$$\varphi_{\rm g}(\lambda) = 2\pi \cdot (n^{g}_{\rm eff} \cdot 2h + d)/\lambda + \Delta\varphi_{\rm g}, \qquad (5)$$

where $\Delta\varphi_{\rm g}$ is an additional phase shift for SPP reflected at the groove ends, $n^{\rm g}_{\rm eff}$ is the refractive index of SPP in the groove. When the phase satisfies $\varphi_{\rm g} = (2m+1)\pi$, $m = 0, 1, 2\ldots$, the minimal intensity in port A is observed, that is, the corresponding transmission wave in channel A is filtered. The filtered wavelength is

$$\lambda_{\rm f} = 2 \cdot (n^{\rm g}_{\rm eff} \cdot 2h + d)/((2m+1) - \Delta\varphi_{\rm g}/\pi). \qquad (6)$$

Assuming that $\Delta\varphi_{\rm g}$ is fixed, $\lambda_{\rm f}$ varies linearly with groove depth h. Changing d has no effect on $n_{\rm eff}^{\rm g}$, namely, the ratio of $\Delta\lambda_{\rm f}/\Delta h$ is fixed, so curves encircled by the dashdot–dot line are parallel and others encircled by the dash line are unparallel due to the influence of groove width on $n_{\rm eff}^{\rm g}$.

4. Conclusion

A unidirectional control of SPP propagation and intensity in the nanocavity has been demonstrated by etching a groove in film 1. It is found that the filtered transmission wave in the cavity is tightly related to the groove shape, while its intensity can be modulated by changing the groove position. The control based on the interference of plasmonic waves is revealed. The groove etched in film 2 works similarly as that in film 1, which makes the design more practical as a device capable of controlling SPP source and intensity with the moveable film 2, and more detailed information about these discussions will be presented in our further work. The present paper provides a clear guideline for harnessing SPPs in the nanocavity and a reference for designing the miniaturized optical devices of filter, splitter, amplifier, etc.

References

[1] Thio T, Lezec H J, Ebbesen T W, Pellerin K M, Lewen G D, Nahata A and Linke R A 2002 *Nanotechnology* **13** 429
[2] Liu B C 2010 *Chin. Phys.* B **19** 9
[3] Ebbesen T W, Lezec H J, Ghaemi H F, Thio T and Wolff P A 1998 *Nature* **39** 667
[4] Cui N, Deng L, Gong S Q, Niu Y P and Wang L C 2010 *Chin. Phys.* B **19** 1
[5] Yang R, Abushagur M A and Lu Z 2008 *Opt. Express* **16** 20142
[6] Lin X S and Huang X G 2008 *Opt. Lett.* **33** 2874
[7] Lin X S and Huang X G 2009 *J. Opt. Soc.* B **26** 1263
[8] Gao H, Shi H, Wang C, Du C, Luo X, Deng Q, Lv Y, Lin X and Yao H 2005 *Opt. Express* **13** 10795
[9] Zhao H, Huang X G and Huang J 2008 *Phys.* E **40** 3025
[10] Veronis G and Fan S 2005 *Appl. Phys. Lett.* **87** 131102
[11] Gan Q Q, Guo B S, Song G F, Chen L H, Fu Z, Ding Y J and Bartoli F J 2007 *Appl. Phys. Lett.* **90** 161130
[12] Gan Q Q, Fu Z, Ding Y J and Bartoli F J 2007 *Opt. Express* **15** 18050
[13] Fu Z, Gan Q Q, Gao K L, Pan Z Q and Bartoli F J 2008 *J. Light Wave Technol.* **26** 3699
[14] Caglayan H and Ozbay E 2008 *Opt. Express* **16** 19091
[15] Choi S B, Park D J, Jeong Y K, Yun Y C, Jeong M S, Byeon C C, Kang J H, Park Q-H and Kim D S 2009 *Appl. Phys. Lett.* **94** 063115
[16] Verslegers L, Catrysse P B, Yu Z F and Fan S H 2009 *Appl. Phys. Lett.* **95** 071112
[17] Zheng G G and Li X Y 2009 *J. Opt.* A: *Pure Appl. Opt.* **11** 075002
[18] Lerosey G, Pile D F P, Matheu P, Bartal G and Zhang X 2009 *Nano Lett.* **9** 327
[19] Wang Y K, Zhang X R, Tang H J, Yang K, Wang Y X, Song Y L, Wei T H and Wang C H 2009 *Opt. Express* **17** 20457
[20] Cetin A E, Guven K and Müstecaphoglu Ö E 2010 *Opt. Lett.* **35** 1980
[21] Taflove A *Computational Electrodynamics: the Finite-Difference Time-Domain Method*, slac, stanford.edu
[22] Cui Y X and He S L 2009 *Opt. Lett.* **34** 16